Soft Matter

RSCPublishing

PAPER

Poly(ethylene oxide)-*block*-poly(*n*-butyl acrylate)-*block*-poly(acrylic acid) triblock terpolymers with highly asymmetric hydrophilic blocks: synthesis and aqueous solution properties†

Petar D. Petrov,*[a] Krassimira Yoncheva,[b] Pavlina Mokreva,[a] Spiro Konstantinov,[b] Juan M. Irache[c] and Axel H. E. Müller[d]

The synthesis and aggregation behaviour in aqueous media of novel amphiphilic poly(ethylene oxide)-*block*-poly(*n*-butyl acrylate)-*block*-poly(acrylic acid) (PEO–P*n*BA–PAA) triblock terpolymers were studied. Terpolymers composed of two highly asymmetric hydrophilic PEO (113 monomer units) and PAA (10–17 units) blocks, and a longer soft hydrophobic P*n*BA block (163 or 223 units) were synthesized by atom transfer radical polymerisation (ATRP) of *n*-butyl acrylate and *tert*-butyl acrylate (*t*BA), followed by selective hydrolysis of the P*t*BA blocks. These terpolymers are not directly soluble in water but form defined spherical micelles by employing the dialysis method as confirmed by dynamic light scattering (DLS) and cryogenic transmission microscopy (cryo-TEM). Based on terpolymer architecture and composition, a three-layered micellar structure comprising a P*n*BA core, a PEO/PAA middle layer, and a PEO outer layer is suggested. The micelles do not dissociate to very low concentrations and, therefore, are promising candidates for long-circulating drug delivery systems. Further, as evidenced by high-performance liquid chromatography (HPLC), the micelles can load and release, without burst effect, the hydrophobic drug paclitaxel.

Introduction

Aggregation of amphiphilic block copolymers into well-defined nanosized structures such as core–shell micelles, vesicles, disks and others in aqueous media is one of their most attractive properties because of possible applications in the very demanding biomedical field.[1–3] For example, the commercially available poly(ethylene oxide)-*block*-poly(propylene oxide)-*block*-poly(ethylene oxide) (PEO–PPO–PEO) triblock copolymers are among the most extensively studied copolymers for the development of drug and gene delivery systems.[4–6] Usually, in water they form spontaneously core–shell micelles above a critical

micellization concentration (cmc) and a critical micellization temperature (cmt) according to the so-called closed association mechanism.[7,8] PEO–PPO–PEO micelles are attractive because they combine good resistance of the PEO shell to protein adsorption and cellular adhesion, the ability of the temperature-responsive PPO core to solubilize water-insoluble compounds and the availability of hydroxyl groups to which receptor-specific ligands can be attached. Since PEO–PPO–PEO micelles are in dynamic equilibrium with molecularly dissolved copolymer chains (unimers), they are, however, very sensitive to changes in concentration and temperature, and may dissociate very fast upon injection into the blood stream.[9] This can lead to the undesired release of the loaded drug before the target is reached (*e.g.* tumor) or the time interval necessary for the specific treatment. The chemical cross-linking of PEO–PPO–PEO micelles is an effective strategy to stabilize them against destructuration and, thus, to prolong their circulation in the body.[9–12] Alternatively, the so-called frozen polymer aggregates are able to maintain their size and morphology upon dilution at very low concentration and from this point of view can be considered as promising long-circulating drug delivery systems.[13] Such aggregates are formed by amphiphilic copolymers comprising usually a hydrophobic block of high glass transition temperature[14,15] or a crystalline polymer[16,17] and are out of equilibrium structures unable to exchange unimers

[a]*Institute of Polymers, Bulgarian Academy of Sciences, Akad. G. Bonchev Str. 103A, 1113 Sofia, Bulgaria. E-mail: ppetrov@polymer.bas.bg; Fax: +359 2 8700309; Tel: +359 2 9796335*

[b]*Department of Pharmaceutical Technology and Biopharmacy, Faculty of Pharmacy, Medical University-Sofia, 2 Dunav Str., 1000 Sofia, Bulgaria. E-mail: krassi.yoncheva@gmail.com; Fax: +359 2 9879874; Tel: +359 2 9236527*

[c]*Department of Pharmacy and Pharmaceutical Technology, University of Navarra, 31080 Pamplona, Spain. E-mail: jmirache@unav.es; Fax: +33 948 425 649; Tel: +33 948 425 600*

[d]*Institute of Organic Chemistry, Johannes Gutenberg University Mainz, Duesbergweg 10-14, D-55128 Mainz, Germany. E-mail: axel.mueller@uni-mainz.de; Tel: +49-6131-39-22372*

† Electronic supplementary information (ESI) available. See DOI: 10.1039/c3sm51144h

within the studied time interval. Interestingly, Colombani *et al.*[18,19] and Jacquin *et al.*[20,21] have found that some aggregates with a liquid poly(*n*-butyl acrylate) (P*n*BA) core and a hydrated poly(acrylic acid) (PAA) shell exhibit behaviour typical for frozen systems, too. This phenomenon is attributed to the high interfacial tension between the hydrophobic P*n*BA blocks and water. Recently, it was reported by our team that asymmetric amphiphilic poly(ethylene oxide)-*block*-poly(*n*-butyl acrylate) (PEO–P*n*BA) diblock copolymers comprising a PEO block of a constant chain length (number-average degree of polymerization DP_n = 113 monomer units) and a longer P*n*BA block (DP_n = 163 or 243) form different aggregates in aqueous media.[22] In particular, $PEO_{113}PnBA_{163}$ forms only spherical "crew-cut" micelles, while $PEO_{113}PnBA_{243}$ forms mainly micelles at a concentration of 0.1 g L^{-1} and unilamellar vesicles at 1.5 g L^{-1}. DLS and FFF analyses revealed that in aqueous media both micelles and vesicles are kinetically "frozen" and do not merge within the experimental time interval. Following the idea that terpolymers of the ABC type are more attractive because the aggregates then combine the intrinsic properties of three components rather than two, we focused our effort on the development of polymer carriers comprising three distinct blocks. In this paper, we report a study on the synthesis and aqueous solution properties of novel amphiphilic PEO–P*n*BA–PAA triblock terpolymers. By design, the length of the PEO block (DP_n = 113) was kept longer than that of the PAA block (DP_n = 10–17). The effect of copolymer composition on the aggregation behaviour was studied in detail using dynamic light scattering, cryogenic transmission electron microscopy and UV-vis measurements. Further, the ability of PEO–P*n*BA–PAA micelles to load and release the hydrophobic anticancer drug paclitaxel was evaluated by HPLC analysis. The cytotoxicity of polymer carriers with and without paclitaxel was assessed as well.

Experimental

Materials

Methoxy poly(ethylene glycol) ($PEO_{113}OH$, MW 5000, Fluka) was precipitated in cold methanol (−40 °C), filtered, and dried under vacuum at 40 °C overnight. *n*-Butyl acrylate and *tert*-butyl acrylate (kindly supplied by BASF AG) were stirred overnight in calcium hydride (Merck, 95%) with an Irganox 1010 inhibitor (CIBA Geigy) and distilled under vacuum. CuBr (Aldrich, 98%) was stirred overnight in glacial acetic acid, filtered, and rinsed successively by acetic acid, ethanol, and ether to remove traces of $CuBr_2$. 2-Bromoisobutyryl bromide (Aldrich, 98%), triethylamine (Fluka, 99.5%), 1,1,4,7,10,10-hexamethyl triethylenetetramine (HMTETA, Aldrich, 98%), *N,N,N′,N′,N″*-pentamethyldiethylenetriamine (PMDETA, Aldrich, 99%), ethyl methyl ketone (Merck, 99.8%), acetone (Aldrich, 99.8%), tetrahydrofuran (THF, Merck, 99.8%), methanol (Merck, 99.8%), 1,4-dioxane (Merck, 99.5%), SiO_2 (63–200 μm, Merck), trifluoroacetic acid (Aldrich, 99%), and 1,6-diphenyl-1,3,5-hexatriene (Aldrich, 98%) were used as received. Dichloromethane (DCM, Aldrich, 99.8%) was stirred overnight in calcium hydride (Merck, 95%) and distilled. Paclitaxel (USP 26 grade, >99.5%) was supplied by 21CEC (London, United Kingdom).

Synthesis

PEO macroinitiator. $PEO_{113}OH$ was reacted with 3 mol equiv. of 2-bromoisobutyryl bromide in dry DCM in the presence of triethylamine (3 mol equiv.) for 24 h at 20 °C. The reaction mixture was then filtered to remove the insoluble hydrobromide salt and then DCM was evaporated. The product was dissolved in THF; the macroinitiator was precipitated in cold methanol (−40 °C), recovered by filtration, and dried under vacuum at 50 °C.

PEO–P*n*BA diblock copolymers. As a typical example, a $PEO_{113}Br$ macroinitiator (1,7448 g, 0.3388 mmol) was dissolved in ethyl methyl ketone (14.8 mL) and degassed using dry nitrogen under stirring for 45 min. Then, the freshly distilled and degassed monomer *n*BA (29.63 mL, 0.207 mol), the HMTETA ligand (0.046 mL; 0.1694 mmol), and the CuBr catalyst (0.0243 g; 0.1694 mmol) were added. The polymerization was carried out at 70 °C for 30 h (40% conversion). Purification was achieved by the precipitation of the reaction mixture in cold methanol (−40 °C) and filtration. The copolymer was redissolved in THF and passed through a silica column to remove the Cu(II) catalyst. Finally, THF was evaporated under vacuum; the copolymer was dissolved in dioxane and freeze-dried.

PEO–P*n*BA–P*t*BA triblock terpolymers. In a typical procedure, a $PEO_{113}PnBA_{223}$–Br macroinitiator (1.1253 g, 0.0333 mmol) was dissolved in acetone (3 mL). This solution was degassed by bubbling nitrogen under stirring for 45 min and then the PMDETA ligand (0.007 mL; 0.0333 mmol), the CuBr catalyst (0.0048 g; 0.0333 mmol), and the freshly distilled and degassed *t*BA monomer (0.195 mL, 1.332 mmol) were added. Polymerization was carried out at 50 °C for 71 h (42% conversion). Purification was achieved by precipitation of the reaction mixture in cold methanol (−40 °C) and filtration. The terpolymer was redissolved in THF and passed through a silica column to remove the Cu(II) catalyst. Finally, THF was evaporated under vacuum; the terpolymer was dissolved in dioxane and freeze-dried.

PEO–P*n*BA–PAA triblock terpolymers. PEO–P*n*BA–P*t*BA terpolymers were dissolved in freshly dried and distilled CH_2Cl_2, followed by the addition of a 15-fold molar excess of CF_3COOH (with respect to the amount of the *tert*-butyl groups). The reaction mixture was stirred at room temperature for 60–65 h, before being precipitated in cold methanol (−40 °C) and filtered. Finally, the terpolymer was dissolved in dioxane and freeze-dried.

Copolymer characterization

Nuclear magnetic resonance spectrometry. ^{1}H NMR spectra were recorded in $CDCl_3$ using a 250 MHz Bruker AC-spectrometer. The DP_n of P*n*BA was calculated by comparing the peak integrals assigned to the PEO protons (4H, –O–C*H*$_2$–C*H*$_2$–) at 3.64 ppm, to the P*n*BA protons at δ = 4.03 (2H, –O–C*H*$_2$–) and at δ = 0.91 (3H, O–CH$_2$–CH$_2$–CH$_2$–C*H*$_3$). The DP_n of P*t*BA was calculated on the basis of peak integrals assigned to the PEO protons (4H, –O–C*H*$_2$–C*H*$_2$–) at 3.64 ppm, to the P*n*BA protons at δ = 4.03 (2H, –O–C*H*$_2$–), δ = 1.2–2 ppm (4H, O–CH$_2$–C*H*$_2$–C*H*$_2$–CH$_3$) and (2H, –C*H*$_2$–C(C=O)H–), and to the *t*BA protons at δ = 1.53 (2H, –C*H*$_2$–C(C=O)H–) and δ = 1.44 (9H, O–C(C*H*$_3$)$_3$).

Gel permeation chromatography. GPC measurements were performed with PSS SDV-gel columns (5 μm, 60 cm, 1 × linear (10^2–10^5 Å), 1 × 100 Å) with THF as the eluent (flow rate = 1.0 mL min^{-1}), at room temperature, and using refractometry for detection. The molar masses and polydispersity index (PDI) were determined using PtBA universal calibration.

Preparation and characterization of aggregates

Sample preparation. PEO–PnBA diblock copolymers and PEO–PnBA–PAA triblock terpolymers were dissolved in dioxane, filtered through a nylon filter with a pore size of 0.1 μm, transferred to a regenerated cellulose tubular membrane ("Spectrum Labs", MWCO 6000–8000 g mol^{-1}), and subsequently dialyzed against Millipore water for several days. In the case of PAA-containing samples, the pH of water was adjusted to 9 by adding NaOH.

Dynamic light scattering. DLS was performed on an ALV DLS/SLS-SP 5022F compact goniometer system with an ALV 5000/E correlator and a He–Ne laser ($\lambda = 632.8$ nm) at scattering angles from 30 to 150° at 25 °C. The normalized intensity autocorrelation function $g^2(t)$ was measured experimentally. The CONTIN method was used for the data analysis of $g^2(t)$. The diffusion coefficient D was calculated from the second moment of each peak as $D = \Gamma/q^2$, where q is the magnitude of the scattering vector ($q = 4\pi n \sin(\theta/2)/\lambda$) and $\Gamma = 1/\tau$ is the relaxation rate. The intensity weighted hydrodynamic radii (R_h) were calculated from the corresponding decay times (τ) by applying the Stokes–Einstein equation: $R_h = k_B T/(6\pi\eta D)$, where η, k_B, and T are the solvent viscosity, the Boltzmann constant, and the absolute temperature, respectively. All samples were measured without filtration. Polydispersity index (PDI = μ_2/Γ^2) was calculated by cumulant analysis. For the monomodal particle size distribution, the cumulant fitting generates reliable values.

Cryogenic transmission electron microscopy. The samples were analyzed by cryo-TEM without filtration. A drop of the dispersion was deposited on an untreated bare copper TEM grid (600 mesh, Science Services), where most of the liquid was removed with blotting paper, leaving a thin film stretched over the grid holes. The specimens were instantly shock vitrified by rapid immersion into liquid ethane cooled at *ca.* 90 K by liquid nitrogen in a temperature-controlled freezing unit (Zeiss Cryobox, Zeiss NTS GmbH). The temperature was monitored and kept constant in the chamber during all of the sample preparation steps. After vitrification, the remaining ethane was removed from the specimen using blotting paper. The specimen was inserted into a cryo-transfer holder (CT3500, Gatan) and transferred to a Zeiss EM922 EF-TEM instrument (Zeiss NTS GmbH). The observations were carried out at *ca.* 90 K. The TEM was operated at an acceleration voltage of 200 kV. Zero-loss filtered images ($\Delta E = 0$ eV) were taken under reduced dose conditions (approximately 100–1000 e nm^{-2}). All images were recorded digitally by a bottom-mounted CCD camera system (Ultrascan 1000, Gatan) and combined and processed with a digital imaging processing system (Digital Micrograph 3.10 for GMS 1.5, Gatan).

UV-vis measurements. UV-vis absorption spectra were recorded in the 250–600 nm range using a DU 800 spectrophotometer (Beckman Coulter). The samples were prepared as follows: 20 μL 1,6-diphenyl-1,3,5-hexatriene (DPH), dissolved in methanol (0.4 mM), was added to 2 mL aqueous dispersions of micelles (0.5 and 0.0075 g L^{-1}) and the samples were incubated in the dark for 16 h at room temperature. The measurements were performed at 20 °C.

Loading of micelles with paclitaxel. Polymers were dissolved in 10 mL of dioxane (concentration 1 g L^{-1}) and paclitaxel (1 mg) was added to this solution under stirring (700 rpm). After incubation for 1 h, 5 mL of purified water was added dropwise. The dioxane was evaporated under reduced pressure (Buchi-144, Switzerland) and the resulting micellar dispersion was filtered (Nylon, 0.22 μm). The filter was rinsed with ethanol and the collected fraction was determined as non-encapsulated paclitaxel by the HPLC method. The aqueous dispersion containing paclitaxel loaded micelles was lyophilized (Genesis 12EL, Virtis, USA) using sucrose as a cryoprotector (5% w/v).

***In vitro* release study.** *In vitro* release of paclitaxel from the micelles was examined in a phosphate buffer (pH 7.4). The freshly prepared micellar dispersion was introduced into a dialysis membrane bag (MW = 6000–8000) that further was placed into 100 mL of phosphate buffer. The release medium was stirred (50 rpm) and the temperature was maintained constantly during the study (37 °C). At predetermined time intervals, the samples were withdrawn from the medium outside the dialysis bag and the concentration of the released paclitaxel was determined by HPLC analysis. HPLC chromatography was performed on an Agilent 1100 series (Waldbronn, Germany), coupled with a UV diode array detection system. The separation of paclitaxel was carried out at 30 °C on a reversed-phase 150 × 3 mm C18 Phenomenex Gemini column (particle size 5 μm). The mobile phase, pumped at 0.5 mL min^{-1}, was 50 : 50 acetonitrile–phosphate buffer (0.02 M, pH = 2.0) and the effluent was monitored by UV detection at 228 nm. For the calculations, the standard curve of paclitaxel was prepared in the 1.25–80.0 μg mL^{-1} concentration range ($r > 0.9991$). The limit of quantification was calculated as 40 ng mL^{-1} with a relative standard deviation of 5.2%.

Determination of the *in vitro* cytotoxic activity of paclitaxel. The activity of paclitaxel loaded in the micelles was evaluated using breast carcinoma MCF-7 cells provided from DSMZ in Braunschweig (Germany). Free paclitaxel was studied using the same line as a reference. The cells were cultivated in RPMI-1640 medium supplemented with L-glutamine and pre-selected 10% fetal bovine serum. For the experiments, logarithmically growing cells were seeded in 96 flat bottomed tissue culture plates (100 μL cell suspension per well at a density of 3 × 10^5 cells per mL). After 24 h cultivation under standard conditions (37 °C under a humidified atmosphere with 5% CO$_2$), stock solutions were added in order to obtain the final paclitaxel concentrations indicated in the results. The incubation time was 72 h and thereafter MTT-dye reduction assay was performed. Briefly, 10 μL of the MTT-solution was added to each well and the plates were further incubated for 4 h at 37 °C. Later, formazan crystals were dissolved by the addition of 5% formic

acid in 2-propanol and absorption was measured at 540 nm using a computerized ELISA reader.

Results and discussion

Synthesis of PEO–PnBA–PAA triblock terpolymers

The terpolymers were synthesized by atom transfer radical polymerization employing the macroinitiator technique (Fig. 1).[23]

First, a PEO_{113}–Br macroinitiator was synthesized by reacting methoxy-PEG (MW 5000) with 2-bromoisobutyryl bromide (BIB) as described elsewhere.[22,24] The polymerization of n-butyl acrylate, initiated by PEO_{113}–Br, was carried out in the presence of the CuBr/HMTETA catalyst system in ethyl methyl ketone. Monomer conversion was monitored by ^{1}H NMR. Polymerization was terminated at ca. 40% conversion of nBA in order to avoid termination reactions like chain–chain coupling and, thus, to minimize the loss of Br end groups. The PEO–PnBA diblock copolymers obtained (Table 1) were purified by precipitation in cold methanol and passed through a silica gel column to remove traces of Cu. Then, PEO–PnBA–PtBA triblock terpolymers were obtained by initiating the polymerization of tert-butyl acrylate with the PEO–PnBA–Br macroinitiator in the presence of the CuBr/PMDETA catalytic system in acetone. It is noteworthy that the polymerization rate was rather slow due to

the low monomer concentration in the reaction mixture dictated by the high molar mass of the macroinitiator. Finally, PtBA blocks were derivatized into PAA blocks by hydrolysis with 15 equiv. of trifluoroacetic acid with respect to the tBA units according to a procedure known to preserve the PnBA groups.[18,19] We found that for the complete hydrolysis of PtBA, the reaction time (Table 1) has to be extended as compared to other reported protocols.[18,25]

The number-average degrees of polymerization of PnBA and PtBA were determined by ^{1}H NMR analysis taking into account that the peak integral of the methylene protons of PEO at 3.64 ppm corresponds to 450 protons. The DPn of PnBA was calculated by comparing the integrals assigned to the PEO protons (Fig. 2, denoted with (a)) to the PnBA protons at 4.03 ppm and 0.91 ppm (Fig. 2, d and g) (see also the Experimental section). The DP_n of PtBA was determined on the basis of the integral difference in the 1.2–2 ppm range from PEO–PnBA and PEO–PnBA–PtBA spectra. The calculated copolymer compositions are very close to the target compositions, indicating good control over the polymerization of nBA and tBA.

^{1}H NMR also provided direct evidence for the efficient conversion of PtBA into PAA. The characteristic peak of the tert-butyl group at $\delta = 1.44$ ppm (Fig. 2, h) could not be detected after the hydrolysis of PtBA with trifluoroacetic acid at the reported experimental conditions. As expected, this reaction did not alter the PnBA block. GPC chromatograms (Fig. 3) of all copolymers synthesized show a monomodal distribution and a low polydispersity that indicate the high efficiency of both PEO–Br and PEO–PnBA–Br macroinitiators. The molar masses and polydispersity indices of the diblock copolymer precursors and triblock terpolymers are given in Table 2.

In summary, three narrowly distributed PEO–PnBA–PAA triblock terpolymers having a long middle PnBA block and two shorter outer hydrophilic PEO and PAA blocks were synthesized in a controlled process via the ATRP mechanism.

Aqueous solution properties

In a previous study,[22] we demonstrated that the asymmetric $PEO_{113}PnBA_{163}$ block copolymer forms spherical "crew-cut" micelles in the 0.2–1 g L^{-1} concentration range, while the copolymer with a longer hydrophobic block, $PEO_{113}PnBA_{243}$, forms micelles at a concentration of 0.1 g L^{-1} and unilamellar

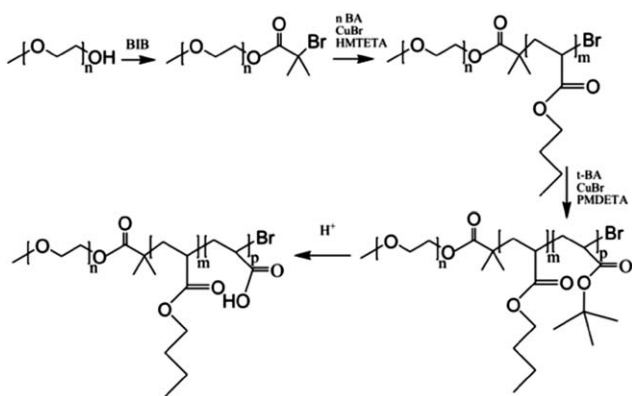**Fig. 1** Schematic pathway of the synthesis of PEO–PnBA–PAA triblock terpolymers via ATRP of nBA and tBA and the subsequent hydrolysis of the PtBA block.

Table 1 Experimental conditions for the synthesis of PEO–PnBA diblock copolymers, PEO–PnBA–PtBA triblock terpolymers, and PEO–PnBA–PAA triblock terpolymers

Target composition	[M] : [I] : [Cu(ı)] : [L]	Reaction temperature (°C)	Reaction time (h)	Monomer conversion/hydrolysis[1]H NMR (%)
$PEO_{113}PnBA_{160}$	400 : 1 : 0.5 : 0.5	70	22	39
$PEO_{113}PnBA_{244}$	610 : 1 : 0.5 : 0.5	70	30	38
$PEO_{113}PnBA_{163}PtBA_{15}$	15 : 1 : 1 : 1	50	73	80
$PEO_{113}PnBA_{163}PAA_{12}$	—	20	65	>99[a]
$PEO_{113}PnBA_{223}PtBA_{10}$	20 : 1 : 1 : 1	50	51	50
$PEO_{113}PnBA_{223}PtBA_{20}$	40 : 1 : 1 : 1	50	71	42
$PEO_{113}PnBA_{223}PAA_{10}$	—	20	60	>99[a]
$PEO_{113}PnBA_{223}PAA_{17}$	—	20	60	>99[a]

[a] The hydrolysis was carried out until the complete disappearance of the characteristic peak of the tert-butyl group at $\delta = 1.44$ ppm.
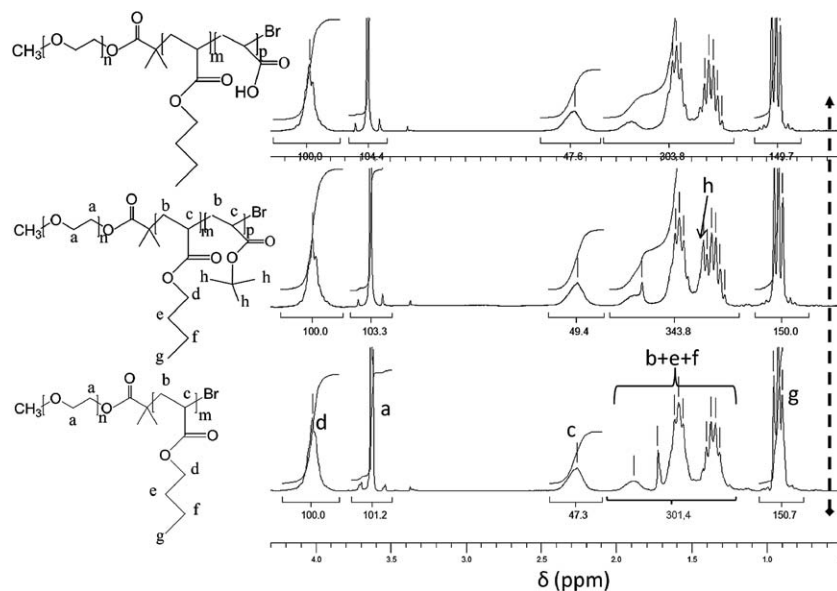
Fig. 2 ^{1}H NMR spectra of PEO$_{113}$PnBA$_{223}$ (bottom), PEO$_{113}$PnBA$_{223}$PtBA$_{17}$ (middle) and PEO$_{113}$PnBA$_{223}$PAA$_{17}$ (top) block copolymers in CDCl$_3$.
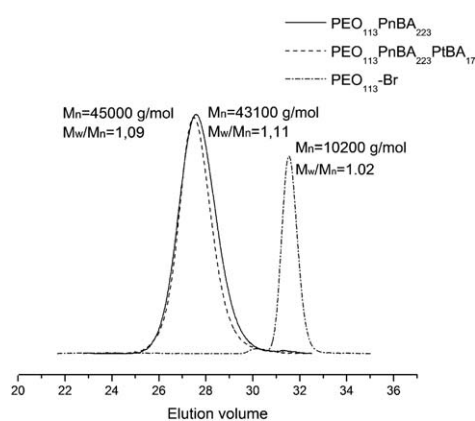
Fig. 3 SEC chromatograms of PEO$_{113}$Br, PEO$_{113}$PnBA$_{223}$ and PEO$_{113}$PnBA$_{223}$PtBA$_{17}$ with THF as the eluent.

vesicles at 1.5 g L^{-1}. Importantly, both copolymers did not spontaneously form aggregates in aqueous media and, therefore, they were first dissolved in dioxane and then dialyzed against water. Here, the same procedure was employed to

prepare aggregates from various PEO–PnBA–PAA triblock terpolymers at a concentration that should favour the formation of micelles (0.2 g L^{-1}). These terpolymers are composed of a hydrophilic PEO block of a constant chain length of 113 monomer units, longer soft hydrophobic PnBA blocks (163 or 223 units), and very short hydrophilic PAA blocks (10–17 units). We assume that the incorporation of a very short PAA block will not significantly alter the ability of copolymers to form core–shell micelles. The dialysis was carried out against basic water (pH 9) to ionize PAA chains and, thus, to avoid complexation with PEO.[25]

The self-assembly of PEO–PnBA–PAA triblock terpolymers was studied by DLS and cryo-TEM. The data for the PEO–PnBA diblock copolymer precursors are included for comparison. All aqueous dispersions were analyzed by DLS at scattering angles ranging from 30 to 150° without filtration. The autocorrelation functions for all dispersions studied were single-exponential and the distributions monomodal. A linear relation of the decay rate, Γ, on q^2 was found which indicates that the aggregates have diffusive behaviour, i.e. the signal registered is from the Brownian motion of the polymer particles (Fig. S1†). In

Table 2 Molecular characteristics of PEO–PnBA–PAA triblock terpolymers, PEO–PnBA diblock copolymer and PEO–PnBA–PtBA triblock terpolymer precursors synthesized by ATRP

Copolymer composition$^{1H\ NMR}$	Mn$^{1H\ NMR}$ (g mol^{-1})	Mn^{GPCa} (g mol^{-1})	PDI^{GPC}	R_h^{90} (nm)	PDI^{DLS}
PEO$_{113}$PnBA$_{163}$	26 000	37 600	1.16	27	0.30
PEO$_{113}$PnBA$_{163}$PtBA$_{12}$	27 500	38 100	1.11	—	
PEO$_{113}$PnBA$_{163}$PAA$_{12}$	26 800	—	—	16	0.19
PEO$_{113}$PnBA$_{223}$	33 800	43 100	1.11	35	0.24
PEO$_{113}$PnBA$_{223}$PtBA$_{10}$	34 900	44 450	1.10	—	
PEO$_{113}$PnBA$_{223}$PtBA$_{15}$	35 500	45 000	1.09	—	
PEO$_{113}$PnBA$_{223}$PAA$_{10}$	34 300	—	—	22	0.18
PEO$_{113}$PnBA$_{223}$PAA$_{15}$	34 700	—	—	22	0.18

^{a} Determined using PtBA universal calibration.

addition, no angular dependence of the apparent translational diffusion coefficient ($D = \Gamma/q^2$) as a function of q^2 (Fig. S2†) is observed, which is typical for isotropic structures with low polydispersity index (PDI).[26] Fig. 4 shows the intensity weighted hydrodynamic radii distribution (CONTIN plot) of triblock terpolymers and diblock copolymer precursors at a scattering angle of $\theta = 90°$.

The hydrodynamic radii calculated by the Stokes–Einstein equation indicate that the detected aggregates are polymeric micelles. The size of the PEO$_{113}$PnBA$_{223}$ micelles is a bit larger than of those prepared from PEO$_{113}$PnBA$_{163}$, which is attributed to the longer hydrophobic block. On the other hand, the existence of very short PAA blocks in the macromolecules of terpolymers definitely leads to a decrease of the micellar size and size distribution (Table 2). Since the length of the PEO blocks is equal and the position and length of the PAA blocks should not contribute to the shrinkage of the shell, the overall reduction of R_h should be attributed to smaller micellar cores. Similar to diblock copolymers, the triblock terpolymers comprising longer PnBA blocks form larger micelles as compared to terpolymers with shorter PnBA blocks.

Aqueous dispersions of diblock copolymers and triblock terpolymers were analysed by cryogenic transmission microscopy, which allows the direct visualisation of the aggregates in their native environment. Cryo-TEM confirmed the formation of spherical micelles (Fig. 5). Undoubtedly, PEO–PnBA–PAA micelles ($D_n = 24 \pm 2$ nm) are smaller than PEO–PnBA micelles ($D_n = 46 \pm 4$ nm). Since the optical density of micellar shells is very similar to that of surrounding water, only the micellar cores are visible. These results are consistent with the DLS measurements and give direct evidence that the smaller size of PEO–PnBA–PAA micelles is due to the smaller size of micellar cores.

On the basis of DLS and TEM data and the terpolymer architecture, we suggest that PEO–PnBA–PAA, similar to PEO–PnBA, aggregates into "crew-cut" core–shell micelles. As the DP$_n$ of PEO (113 units) exceeds significantly that of PAA (10–17 units), a three-layered micellar structure may be anticipated, thus the PnBA core, a PEO/PAA middle layer, and a PEO outer layer (Fig. 6). We assume that the PnBA blocks in triblock terpolymers undergo specific bending caused by the phase
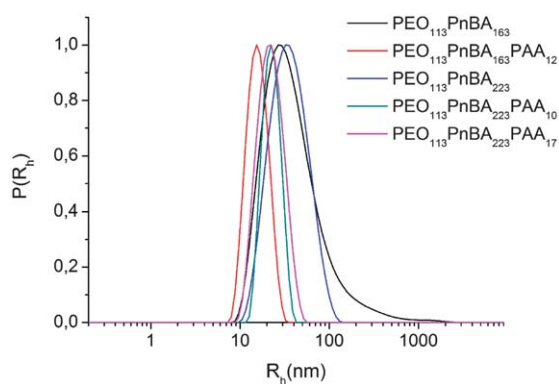

Fig. 5 Cryo-TEM micrographs of polymeric micelles formed by PEO$_{113}$PnBA$_{223}$ diblock copolymers (a) and PEO$_{113}$PnBA$_{223}$PAA$_{17}$ triblock terpolymers (b).

separation of the middle hydrophobic and the two outer hydrophilic segments (Fig. 6, right). Such bending decreases the apparent length of the core forming blocks resulting in the smaller core of the PEO–PnBA–PAA micelles as compared to the PEO–PnBA ones.

Based on previous studies,[25,27] it is supposed that the two hydrophilic blocks are randomly dispersed within the middle layer. The outer PEO layer is supposed to protect the micelles from clearance by the reticuloendothelial system from the blood stream at an early stage.[28] PAA chains in the middle layer provide the system with additional functionality and potential for binding, for example, metal ions.[25]

As pointed out in the Introduction, the structural integrity of micelles upon intravenous injection into an animal or human subject is a key factor for determining the applicability of a given system for drug delivery. Following a standard protocol, Allen et al. suggested that the injection of a micellar dispersion (concentration 2% w/w) will result in a 50-fold decrease of

Fig. 4 Apparent hydrodynamic radii distribution at $\theta = 90°$ of aggregates formed by PEO–PnBA–PAA triblock terpolymers and PEO–PnBA diblock copolymer precursors.
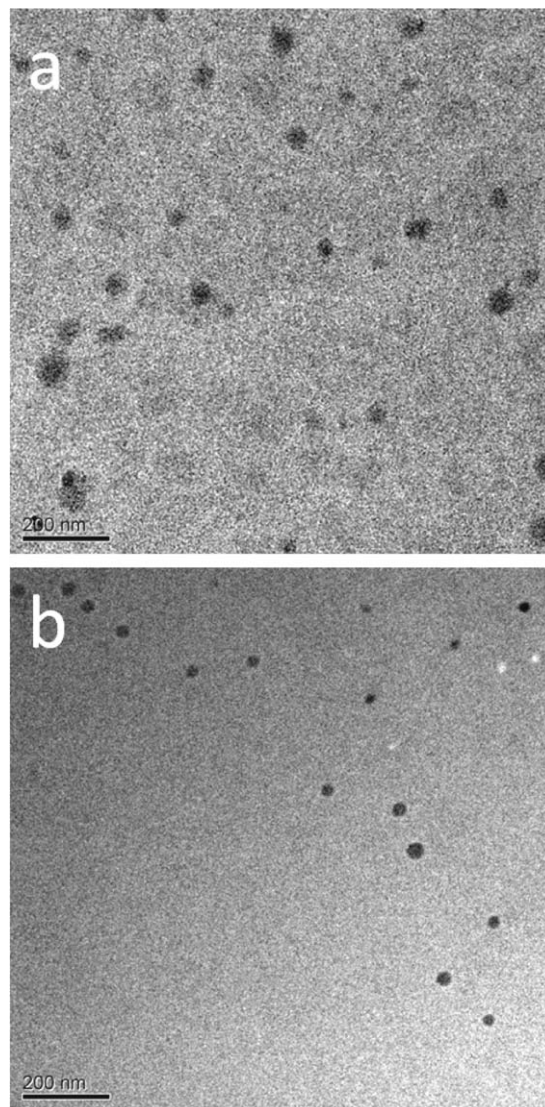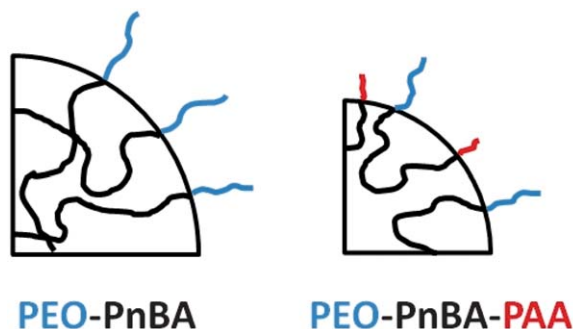
Fig. 6 Schematic illustration of "crew-cut" micelles formed by PEO–PnBA diblock copolymers (left) and PEO–PnBA–PAA triblock terpolymers (right).

copolymer concentration in the blood.[29] From this point of view, it is advantageous to select a copolymer system with a low cmc value. It has been reported that micelles comprising the PnBA core (DP$_n$ of PnBA = 90) have an extremely low cmc (2×10^{-8} mol L^{-1}; 0.45 mg L^{-1}), approaching the lower limit of the methods used for determination.[18] Theoretical calculations show that the cmc values of PnBA–PAA block copolymers dramatically decrease with the increase of the molar mass of PnBA.[20] It is noteworthy that the micellization of such copolymers is considered to be a kinetically controlled process. This statement is in accordance with our observation that polymeric vesicles formed by PEO$_{113}$PnBA$_{246}$ at concentration 1.5 g L^{-1} did not undergo morphological transformation to micelles upon dilution to 0.1 g L^{-1}, although micelles were formed by the same copolymer at a starting concentration of 0.1 g L^{-1}.[22] In this study, we focused on proving whether the polymeric micelles formed by PEO–PnBA–PAA triblock terpolymers maintain their integrity at more than 50-fold dilution. For that purpose, we performed experiments using the hydrophobic dye 1,6-diphenyl-1,3,5-hexatriene (DPH) as a probe indicating the existence of micelles. It is known that DPH can be easily solubilized by the hydrophobic micellar cores, giving a characteristic spectrum with a maximum at 356 nm.[30] Fig. 7 shows the UV-vis spectra of the PEO$_{113}$PnBA$_{163}$PAA$_{12}$/DPH micellar dispersion at
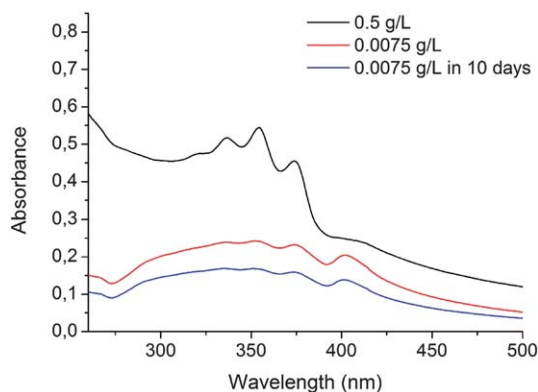
concentrations 0.5 g L^{-1} and 0.0075 g L^{-1} (prepared by 67-fold dilution of the first sample).

Clearly, the sample prepared by dilution exhibits absorbance, indicating that the DPH molecules are located in the hydrophobic micelle interior. Moreover, after 10 days of storage, there is still evidence for the existence of micelles. This result revealed that PEO–PnBA–PAA micelles are resistant upon severe dilution and do not dissociate quickly, which is typical for kinetically frozen systems.

Drug loading and release properties

The ability of PEO–PnBA–PAA micelles to load hydrophobic drugs was tested with paclitaxel (PXL). PXL is an antineoplastic drug successfully used against a variety of tumors, including ovarian, breast and non-small cell lung tumors.[31,32] PXL was incorporated into the micelle core by dissolving both the drug and copolymer in dioxane, dropwise addition of water and the subsequent removal of the organic solvent under vacuum. The incorporation of the drug did not alter remarkably the size of the micelles. Both systems maintained good colloidal stability in phosphate buffer at the reported experimental conditions. The zeta-potential values (Zetamaster analyzer, Malvern Instruments) measured at pH 7.4 for the PEO–PnBA and PEO–PnBA–PAA micelles were -23.5 ± 4 and -29.3 ± 2, respectively. This result indicates that the longer PEO segments could not completely screen the negatively charged shorter PAA blocks. The calculated drug loading and encapsulation efficiency for PEO$_{113}$PnBA$_{163}$PAA$_{12}$ micelles were 8.1% and 85.5%, respectively. For comparison, the above parameters for PEO$_{113}$PnBA$_{163}$ micelles were almost the same, 8.4% and 87%.

In vitro release profiles of paclitaxel from PEO$_{113}$PnBA$_{163}$-PAA$_{12}$ and PEO$_{113}$PnBA$_{163}$ micellar formulations are shown in Fig. 8.

The results revealed a sustained release of paclitaxel in the phosphate buffer without the burst effect. The avoidance of the burst effect is due to the complete incorporation of PXL in the micelle cores. Slower paclitaxel release from the PEO–PnBA–PAA micelles was observed. In particular, 100% of paclitaxel was released after 50 hours from PEO–PnBA micelles, whereas for
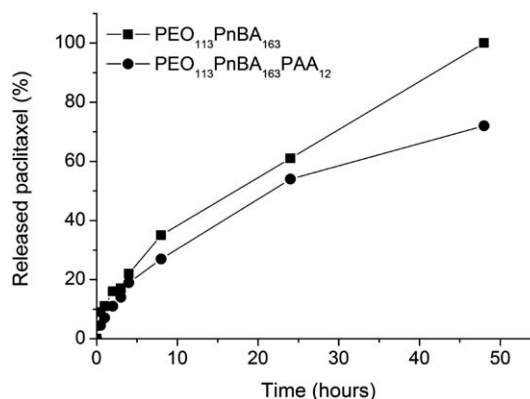

Fig. 7 UV-vis absorption spectra of DPH immobilized in PEO$_{113}$PnBA$_{163}$PAA$_{12}$ micelles in aqueous media.

Fig. 8 *In vitro* release of paclitaxel from PEO$_{113}$PnBA$_{163}$ and PEO$_{113}$PnBA$_{163}$-PAA$_{12}$ micelles in phosphate buffer (pH 7.4).

Table 3 Kinetic analysis of *in vitro* release data obtained for the two paclitaxel loaded micellar formulations

Micelles	Zero-order	Higuchi model
PXL–PEO$_{113}$PnBA$_{163}$	$r = 0.9695$	$r = 0.9892$
PXL–PEO$_{113}$PnBA$_{163}$PAA$_{12}$	$r = 0.9314$	$r = 0.9961$
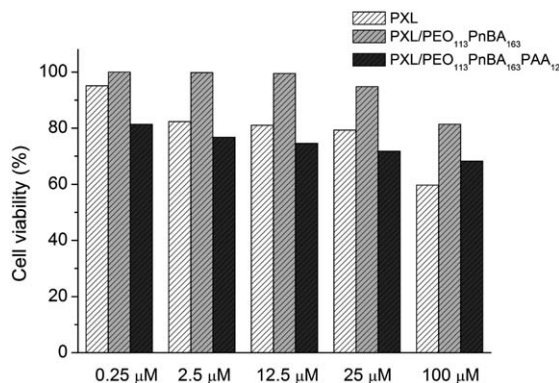
Fig. 9 *In vitro* cytotoxicity of free paclitaxel and paclitaxel loaded micelles in breast carcinoma MCF-7 cells.

the same time, approximately 70% of the drug was released from PEO–PnBA–PAA micelles. The drug loading of the micelles was similar suggesting that the different release pattern is probably due to the different properties of micelle shells. One can speculate that the presence of the PEO/PAA middle layer increases the segmental density at the interface which slows down the diffusion of drug molecules.

Kinetic analysis of *in vitro* release data showed higher correlation with the Higuchi diffusion model than the zero-order model (Table 3, Fig. S3†).[33] Thus, the diffusion process is considered as the main mechanism of paclitaxel release.

The cytotoxicity of polymeric carriers, paclitaxel loaded micelles and free paclitaxel was investigated in breast carcinoma MCF-7 cells. Polymeric carriers showed no cytotoxicity in the selected cells. Further, different cytotoxicities of paclitaxel loaded micellar formulations were observed (Fig. 9). In particular, paclitaxel loaded PEO$_{113}$PBA$_{163}$PAA$_{12}$ micelles possessed higher cytotoxicity compared to PEO$_{113}$PBA$_{163}$ micelles. Paclitaxel loaded PEO$_{113}$PBA$_{163}$PAA$_{12}$ micelles showed even higher cytotoxicity than free paclitaxel. In addition, the incubation of paclitaxel loaded PEO$_{113}$PBA$_{163}$PAA$_{12}$ micelles in the cells revealed higher cytotoxicity independent of the dose applied. These results suggest better cellular uptake of these micelles probably due to the eventual interaction of PAA chains with the cell membrane.

Conclusions

PEO–PnBA–PAA triblock terpolymers with controlled composition and narrow molar mass distribution formed defined spherical "crew-cut" micelles in aqueous media with the aid of a co-solvent. As the DP$_n$ of PEO (113 units) exceeded significantly the DP$_n$ of the PAA (10–17 units) block, the formation of a three-layered micellar structure comprising a soft PnBA core, a PEO/PAA middle layer, and a PEO outer layer is suggested. The existence of a third PAA block resulted in the formation of micelles with smaller size and narrower size distribution as compared to the PEO–PnBA micelles. The introduction of PAA chains also imparts additional functionality to the system which could be utilized for the synthesis of AgNP within the micelle templates. The type and length of the hydrophobic block (PnBA; DP$_n$ = 163 or 223) determined an excellent stability of micellar structures upon severe dilution, which, in combination with the ability of PEO–PnBA–PAA micelles to release paclitaxel without the burst effect, makes them a promising candidate for long-circulation drug delivery systems. The potential of PEO–PnBA–PAA micelles as vehicles of both the anti-angiogenic drug and AgNPs could be further explored for achieving a synergistic effect on the inhibition of tumor growth.

Acknowledgements

Notes and references

1 G. Riess, *Prog. Polym. Sci.*, 2003, **28**, 1107.
2 L. Zhang and A. Eisenberg, *Science*, 1995, **268**, 1728.
3 I. W. Hamley, in *Block Copolymers in Solution: Fundamentals and Applications*, ed. I. W. Hamley, John Wiley, Chichester, 2005, p. 7.
4 A. V. Kabanov, E. V. Batrakova and V. Yu. Alakhov, *J. Controlled Release*, 2002, **82**, 189.
5 A. V. Kabanov, P. Lemieux, S. Vinogradov and V. Alakhov, *Adv. Drug Delivery Rev.*, 2002, **54**, 223.
6 V. P. Torchilin, *J. Controlled Release*, 2001, **73**, 137.
7 P. Alexandridis, J. F. Holzwarth and T. A. Hatton, *Macromolecules*, 1994, **27**, 2414.
8 K. Mortensen and J. S. Pedersen, *Macromolecules*, 1993, **26**, 805.
9 N. Rapoport, *Colloids Surf., B*, 1999, **16**, 93.
10 G. Husseini, D. Christensen, N. Rapoport and W. G. Pitt, *J. Controlled Release*, 2002, **83**, 303.
11 P. Petrov, M. Bozukov and Ch. B. Tsvetanov, *J. Mater. Chem.*, 2005, **15**, 1481.
12 K. Yoncheva, P. Calleja, M. Agüeros, P. Petrov, I. Miladinova, Ch. Tsvetanov and J. M. Irache, *Int. J. Pharm.*, 2012, **436**, 258.
13 T. Nicolai, O. Colombani and C. Chassenieux, *Soft Matter*, 2010, **6**, 3111.
14 I. Astafieva, X. F. Zhong and A. Eisenberg, *Macromolecules*, 1993, **26**, 7339.
15 L. Zhang and A. Eisenberg, *J. Am. Chem. Soc.*, 1996, **118**, 3168.
16 L. Yin and M. A. Hillmyer, *Macromolecules*, 2011, **44**, 3021.

17 H. Freichels, R. Auzély-Velty, P. Lecomte and C. Jérôme, *Polym. Chem.*, 2012, **3**, 1436.

18 O. Colombani, M. Ruppel, F. Schubert, H. Zettl, D. Pergushov and A. H. E. Müller, *Macromolecules*, 2007, **40**, 4338.

19 O. Colombani, M. Ruppel, M. Burkhardt, M. Drechsler, M. Gradzielski, M. Schumacher and A. H. E. Müller, *Macromolecules*, 2007, **40**, 4351.

20 M. Jacquin, P. Muller, R. Talingting-Pabalan, H. Cottet, J. F. Berret, T. Futterer and O. J. Theodoly, *J. Colloid Interface Sci.*, 2007, **316**, 897.

21 M. Jacquin, P. Muller, H. Cottet, R. Crooks and O. Theodoly, *Langmuir*, 2007, **23**, 9939.

22 P. D. Petrov, M. Drechsler and A. H. E. Müller, *J. Phys. Chem. B*, 2009, **113**, 4218.

23 K. Matyjaszewski and J. Xia, *Chem. Rev.*, 2001, **101**, 2921.

24 K. Jankova, X. Chen, J. Kops and W. Batsberg, *Macromolecules*, 1998, **31**, 538.

25 P. Petrov, Ch. B. Tsvetanov and R. Jérôme, *J. Phys. Chem. B*, 2009, **113**, 7527.

26 D. Lehner, H. Lindner and O. Glatter, *Langmuir*, 2000, **16**, 1689.

27 T. Miyoshi, K. Takegoshi and K. Hikichi, *Polymer*, 1997, **38**, 2315.

28 G. S. Kwon and T. Okano, *Adv. Drug Delivery Rev.*, 1996, **21**, 107.

29 C. Allen, D. Maysinger and A. Eisenberg, *Colloids Surf., B*, 1999, **16**, 3.

30 P. Alexandridis, J. F. Holzwarth and T. A. Hatton, *Macromolecules*, 1994, **27**, 2414.

31 R. E. Gregory and A. F. DeLisa, *Clin. Pharm.*, 1993, **12**, 401.

32 Q. Chen, Q. Z. Zhang, J. Liu, L. Q. Li, W. H. Zhao, Y. J. Wang, Q. H. Zhou and L. Li, *Chinese Journal of Oncology*, 2003, **25**, 190.

33 P. Costa and J. M. S. Lobo, *Eur. J. Pharm. Sci.*, 2001, **13**, 123–133.